Available online at www.sciencedirect.com
SCIENCE DIRECT
Journal of Photochemistry and Photobiology A: Chemistry 177 (2006) 177–184
Journal of Photochemistry and Photobiology A:Chemistry
www.elsevier.com/locate/jphotochem

Electrochemically synthesized CdS nanoparticle-modified TiO_2 nanotube-array photoelectrodes: Preparation, characterization, and application to photoelectrochemical cells

Siguang Chen [a], Maggie Paulose [a], Chuanmin Ruan [a], Gopal K. Mor [a], Oomman K. Varghese [a], Dimitris Kouzoudis [b], Craig A. Grimes [a,*]

[a] *Department of Electrical Engineering, Department of Materials Science and Engineering, The Materials Research Institute, The Pennsylvania State University, University Park, PA 16802, USA*
[b] *Department of Engineering Science, University of Patras, 26504 Patras, Greece*

Received 20 April 2005; received in revised form 18 May 2005; accepted 18 May 2005
Available online 24 June 2005

Abstract

A novel electrodeposited CdS nanoparticle-modified highly-ordered TiO_2 nanotube-array photoelectrode and its application to photoelectrochemical cells is reported. Results show formation of a thin, nanoparticulate CdS layer, comprised of sphere-like 10–20 nm diameter nanoparticles, on the anodic synthesized TiO_2 nanotube-array (inner diameter of 70 nm, wall thickness 25 nm and ca. 400 nm length) electrode. The resulting CdS–TiO_2 photoelectrode has an as-fabricated bandgap of 2.53, and 2.41 eV bandgap after sintering at 350 °C in N_2 ambient. Photoelectrochemical properties are described in detail.

Keywords: CdS nanoparticle; TiO_2 nanotube-array; Photoelectrochemical; Photoelectrode

1. Introduction

Nano-dimensional titanium oxide has received considerable attention over the past two decades in photovoltaic and photocatalysis applications [1–7]. We have previously reported the synthesis of unique, highly ordered TiO_2 nanotube-arrays and their application to hydrogen gas sensing [8], as well as water splitting [9]. When TiO_2 nanotube-arrays are used as photoanodes, under 320–400 nm illumination, the efficiency of hydrogen generation by photolysis can reach a remarkable 12.8% with a normalized hydrogen generation rate of 80 mL/W h [10]. There are at least two obvious reasons for the excellent photoelectrolysis properties. The first is that the highly ordered thin-wall TiO_2 nanotube-array facilitates kinetic separation of photogenerated charge in photoelectrochemical applications [10]. The other is that the TiO_2 nanotube-array is anodically synthesized from Ti foil, thus after annealing the TiO_2 nanotube array has a direct, high quality Ohmic contact with the underlying electrically conductive Ti substrate. Our early results [9,10] show that the highly-ordered nanotube array architecture is promising for photoelectrochemical (PEC) applications. However, as is well known the band gap of TiO_2 (3.2 eV) limits the absorption of sunlight to the ultraviolet region of the solar spectrum. Considerable work by many investigators has focused on improving the absorption of visible light of TiO_2 nanocrystalline for PEC cells by incorporation of substitutional atoms into the lattice, including both non-metal [11] and metal atoms [12]. Although this incorporation of substitutional atoms improves the visible light absorption in TiO_2 electrodes, they have not yet proven suitable for efficient PEC cell application.

Other efforts concerned with band-gap shifting of TiO_2 have focused on the sensitization of TiO_2 photoelectrodes by combining them with narrow-bandgap semiconductor films

* Corresponding author. Tel.: +1 814 865 9142; fax: 1 814 865 6780.
E-mail address: cgrimes@engr.psu.edu (C.A. Grimes).

1010-6030/$ – see front matter © 2005 Elsevier B.V. All rights reserved.
doi:10.1016/j.jphotochem.2005.05.023

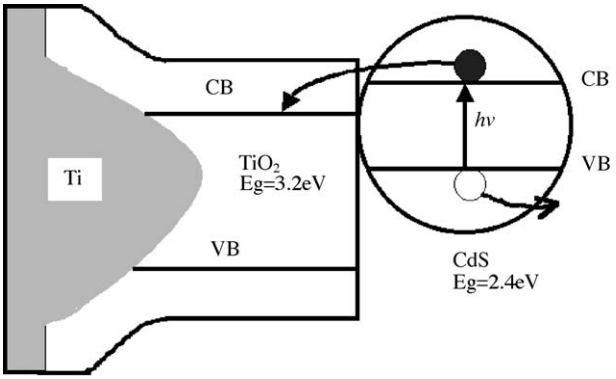

Fig. 1. Schematic diagram illustrating charge injection from excited CdS into TiO_2. CB and VB refer to the energy levels of the conduction and valence bands, respectively, of CdS particle and TiO_2 nanotube wall.

[13]. Such sandwich electrodes may be advantageous as electron injection may be optimized through confinement effects, and a sensitizer, a 1.5 eV edge absorber, is well approximated by a narrow bandgap semiconductor material [14]. Since the conduction band of bulk CdS is ca. 0.5 V more negative than that of TiO_2, the coupling of the semiconductors should have a beneficial role in improving charge separation as shown in Fig. 1; excited electrons from the CdS nanoparticles can quickly transfer to the TiO_2 nanotube-array, see Fig. 2, arriving at the photocurrent collector through the highly ordered nanotube-array structure. The self-assembled, highly-ordered nanotube-array structure made by anodization of titanium is evident in Fig. 2. In cross section, the nanotube-array rests upon a titania barrier layer [8], intrinsic to the anodization process, that separates the nanotube-array from the underlying titanium substrate, e.g. the portion of the initial titanium foil that is not anodized.

Early studies on the combination of TiO_2 with CdS include that of Weller and co-workers [15], who reported excellent visible-spectrum properties of a photocell made by the combination of in situ prepared CdS particles (4–20 nm) with a highly porous nanocrystalline TiO_2 electrode. Kohtani et al. [16] reported deposition of CdS microcrystals onto a TiO_2 semiconductor; they found that the resulting PEC properties, such as flat band potential, were strongly influenced by the CdS sensitizer. Kamat and co-workers [17] used reverse micelle synthesized quantum-sized CdS and TiO_2 particles, finding that electron transfer from photoexcited CdS to TiO_2 strongly depended on the TiO_2 particle size. Fitzmaurice and co-workers [18] prepared CdS–TiO_2 electrodes and studied the conduction band of TiO_2, CdS, and CdS–TiO_2 sandwich electrodes, and their potential for use in regenerative photoelectrochemical cells, by potential dependent spectroscopy. More recently, Bai et al. [19] prepared TiO_2–CdS composite nanotubes via a Layer-by-Layer assembly technique, in combination with a nanoporous alumina template, with the resulting nanotubes exhibiting a novel PL band in the blue-wavelength range. Other efforts to modify TiO_2 nanoparticle electrodes by CdS include self-assembly techniques

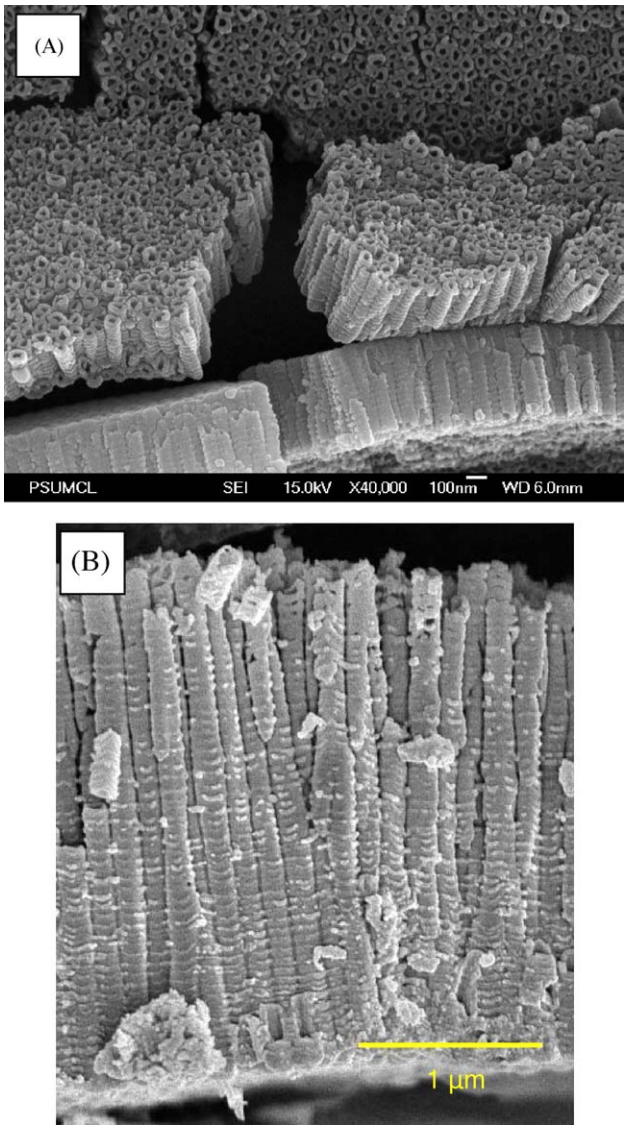

Fig. 2. Illustrative TiO_2 nanotube array film made by anodization of a titanium foil, (A) after intentional cracking for imaging of cross-section, and (B) cross-sectional image showing nanotube-array atop barrier layer at bottom of nanotubes. The nanotube-array rests upon a titania barrier layer [8] that separates the nanotube-array from the underlying titanium substrate, from which these samples have been removed for FE-SEM imaging.

[20–22], electrochemical synthesis in aqueous solution [23], and chemical bath deposition [24].

We seek to combine the excellent photochemical properties of the crystalline TiO_2 nanotube-arrays with the excellent visible absorption properties of CdS nanoparticles, thereby shifting the absorption characteristics of the material architecture into the visible light spectrum. To date there are no reports on modification of these highly-ordered, self-assembled TiO_2 nanotube-arrays using CdS, or indeed any dopant, for application in photoelectrochemical cells. Consequently this work examines a novel TiO_2 nanotube-array photoelectrochemical cell photoanode modified by coating with an electrochemically synthesized

CdS-nanoparticle film, deposited by cathodic reduction of Cd^{2+} from a non-aqueous solvent containing sulfur in elemental form [17,25–27]. The photoelectrochemical properties of the TiO_2 nanotube-array photoelectrodes before and after CdS nanoparticle-modification are described in detail.

2. Experimental

2.1. Chemicals and instruments

High-purity titanium foil (99.7%) with 0.25 mm thickness, 48–52% HF, 52% Acetic acid, $CdCl_2$, a Cd rod 2 mm in diameter, Sulfur, Na_2S, were purchased from Aldrich and used as delivered without further purification. A Kratos Analytical Axis Ultra XPS, Philips X'pert MRD PRO X-ray diffractometer (Almelo, The Netherlands), Universal V3.0G TGA Instruments, HP 8452 UV–vis spectrophotometer, and JEOL JSM6300 field emission SEM were used to investigate the structure and properties of the prepared electrodes.

2.2. Preparation of electrochemically synthesized CdS-modified TiO_2 nanotube-array electrode

TiO_2 nanotube electrodes were prepared in a HF and acetic acid solution using anodic oxidation, as described in [28]. Titanium foil samples, 2.5 cm × 1.0 cm, were immersed in a mixed solution of 0.05% HF and 13% acetic acid, and applied to a constant 20 V anodic potential for 45 min (23 °C). After anodic oxidation, the samples were immediately rinsed with D.I. water, and then dried in a N_2 stream. The resulting amorphous titania nanotube arrays were annealed at 480 °C for 6 h with heating and cooling rates of l °C/min in an O_2 atmosphere to crystallize the tube walls and improve the stoichiometry.

A CdS film was then deposited upon the crystallized TiO_2 nanotube-array by cathodic reduction, using a conventional three-electrode system comprising an Ag/AgCl reference electrode and Cd counter electrode. A mixed solution of saturated elemental sulfur in benzene with 0.6 M $CdCl_2$ in dimethyl sulfoxide (DMSO) was used as the electrolyte. The solution was bubbled with flowing N_2 for 30 min prior to electro-deposition in order to remove O_2 and any moisture within the solution. The cathodic potential was kept constant at −0.5 V for different deposition times. After electrodeposition the samples were thoroughly rinsed with acetone, methanol and D.I. water. The prepared CdS–TiO_2 electrodes were annealed at 350 and 400 °C for 60 min in a N_2 atmosphere to investigate the influence of annealing on their photoelectrochemical response. We suggest that when a cathodic potential is applied to the TiO_2 nanotube electrode, it will reduce sulfur to S^{2-} on the electrode surface, while the applied electric field induces Cd^{2+} to migrate towards the electrode hence under proper conditions CdS will form at the electrode surface [27]. For comparison, CdS was also electrodeposited on a planar F-doped transparent Tin Oxide (FTO) glass substrate at −0.5 V for 30 min and annealed at 400 °C for 60 min.

2.3. Photoelectrochemical measurements

A HCH Instruments electrochemical analyzer was used to measure the photoelectrochemical response of the samples, with conventional three-electrode system comprising an Ag/AgCl reference electrode and Pt foil counter electrode. A1 M Na_2S aqueous solution was used as the electrolyte. A Spectra Physics Simulator with an illumination intensity of 1 sun (AM 1.5, 100 mW/cm^2) with a filter to remove light of wavelength below 400 nm was used as the light source. A PHIR CE power meter was used to calibrate the input power before and after the photoelectrochemical measurements.

3. Results and discussion

Fig. 3a shows an illustrative FE-SEM image, top surface view, of a TiO_2 nanotube-array upon which just a few CdS nanoparticles, ≈20 nm diameter, have been deposited (−0.5 V for 5 min). The nanotubes have a length of ≈400 nm, and a barrier layer thickness of ≈50 nm; the average pore diameter as calculated from the FE-SEM images was 76 nm with a standard deviation of 15 nm, and wall thickness of 27 nm with a standard deviation of 6 nm. Fig. 3b shows the topology after a 30 min (−0.5 V) electrodeposition of the CdS nanoparticles; the TiO_2 nanotubes have been extensively covered with a relatively uniform layer of CdS nanoparticle 'clumps' ranging in diameter from 40 to 100 nm. Fig. 3c is an illustrative cross-sectional image of CdS electrodeposited sample, −0.5 V for 30 min, that has been freed from the underlying titanium substrate. The barrier layer is to the right, seen as a continuous seam at the edge of the sample. Although it is possible, and indeed likely that some CdS nanoparticles reside within the nanotube arrays we have not been able to detect any using FE-SEM imaging.

The general scan spectrum of XPS over a large energy range at low resolution was used to quickly identify the elements present in the CdS–TiO_2 electrodes, Fig. 4a, with the survey showing sharp XPS peaks for Ti, O, Cd, S, and also C. Fig. 4b and c are, respectively, Cd 3d and S 2p core level XPS scans over smaller energy windows at higher resolution. The Cd 3d core level XPS spectrum (Fig. 4b) has two peaks at 405.3 eV ($3d_{5/2}$) and 411.9 eV ($3d_{3/2}$), in good agreement with published values for CdS [29]. The S 2p core level spectrum, Fig. 4c, indicates that there are two chemically distinct species in the spectrum. The peak at 161.9 eV is for sulfide, the structure occurs because of a split between $2p_{3/2}$ and $2p_{1/2}$; the split is near 1.18 eV and the area ratio is 2:1, in excellent agreement with published values of the S 2p signal for CdS [29]. Thus CdS is identified both from the sulfide peak at 161.9 eV (Fig. 4c), but also from the peak at 411.9 eV of the Cd $3d_{3/2}$ and 405.3 eV of the Cd $3d_{5/2}$ (Fig. 4b) [29].

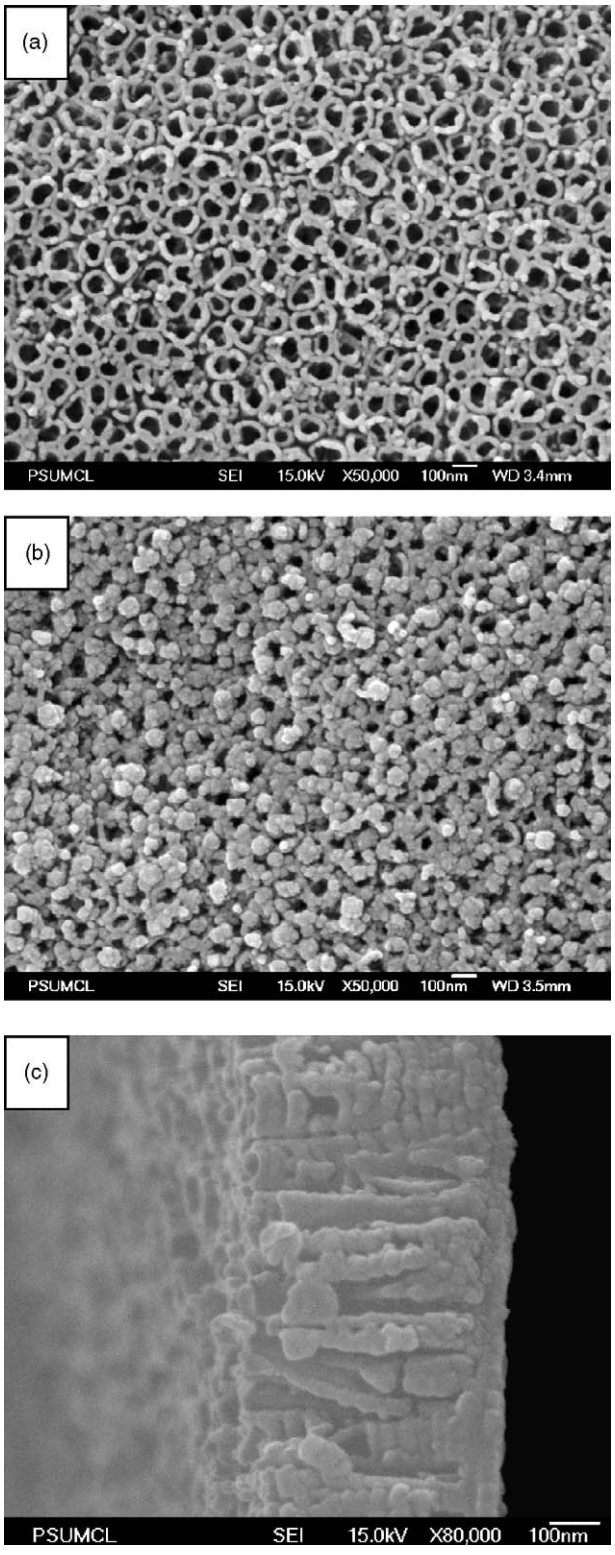

Fig. 3. Top surface FE-SEM view of the prepared CdS–TiO_2 nanotube-array electrode: (a) after CdS electrodeposition at −0.5 V for 5 min, (b) after CdS electrodeposition at −0.5V for 30 min, (c) illustrative cross-sectional image of CdS electrodeposited sample, −0.5 V for 30 min. The barrier layer is to the right, seen as a continuous seam at the edge of the sample.

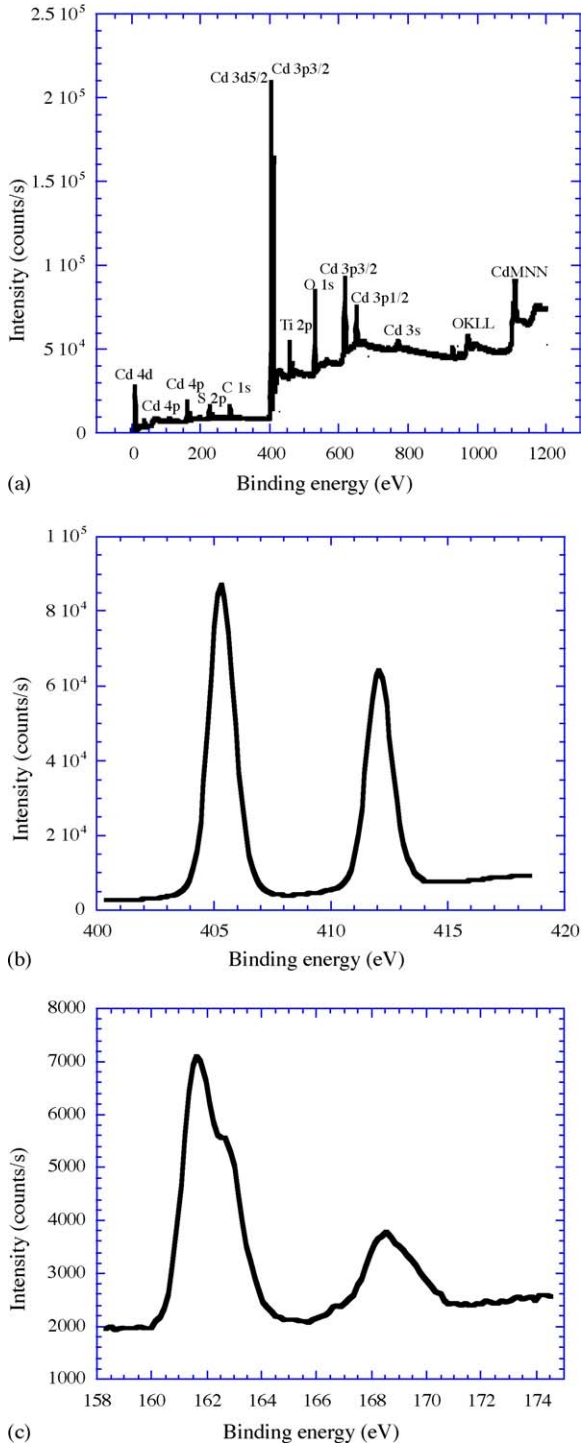

Fig. 4. (a) XPS survey scan for CdS modified TiO_2 nanotube-array electrode over a large energy range at low resolution, the spectra showed Ti, Cd, O, S, C present in the sample, (b) Cd 3d XPS core level spectra of CdS modified TiO_2 nanotube-array electrode, (c) S 2p XPS core level spectra of CdS modified TiO_2 nanotube-array electrode.

The peak at 168.4 eV in S 2p is assigned to Sulfur in sulfate, for reaction with humid environments causes the outer surface of a sulfide to oxidize and form sulfate [30]. Measured atomic concentrations, determined using XPS, of the as-prepared samples are shown in Table 1, with the various

Table 1
Concentration of various elements present in the CdS modified TiO_2 nanotube electrode

Atom	%
O	31.1
Ti	4.2
Cd	25.5
C	16.6
Sulfide	17.1
Sulfate	5.5
Sulfide/Cd	0.86
Sulfate/Cd	1
O/Ti	7.3

ratios of Sulfide/Cd, Sulfate/Cd and O/Ti also tabulated. As observed from Table 1, when the Sulfate/O ratio is 1, the Sulfide/Cd ratio is 0.86; this means that the CdS nanoparticles obtained are slightly Cd rich, which is expected for CdS under normal synthesis conditions [31]. The XPS signal of Ti indicated that not all of the TiO_2 nanotubes are covered by CdS, as was confirmed by the FE-SEM images. The O/Ti ratio seen in Table 1 indicates more oxygen than one would like, however oxygen and carbon are common contaminants found on the surface of many samples [31].

Fig. 5 shows the X-ray diffraction (XRD) pattern of an illustrative CdS modified TiO_2 nanotube array electrode after annealing at 350 °C for 1 h. In addition to the observed prominent TiO_2 Bragg peak [32], there are weak Bragg reflections at 2 theta values of 26.55, 30.75, 44.04, 52.16, 54.67, corresponding to the (1 1 1), (2 0 0), (2 2 0), (3 1 1), and (2 2 2) Bragg reflections of Cubic CdS, respectively (see PCPDS card No. 80-0019). The XRD results confirm formation of CdS on the TiO_2 nanotube-array electrode.

Earlier we reported annealing, as well as TGA and DSC analyses of TiO_2 nanotube-array electrodes in an O_2 ambient; the TiO_2 nanotube-arrays, 480 °C annealed, are anatase [32]. The prepared CdS modified TiO_2 nanotube-array electrode

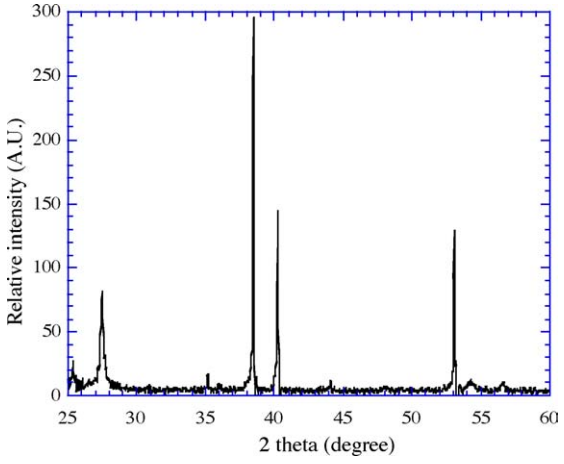

Fig. 5. XRD pattern of CdS on TiO_2 nanotube array electrode; Bragg reflection peaks for cubic CdS are indicated by open squares.

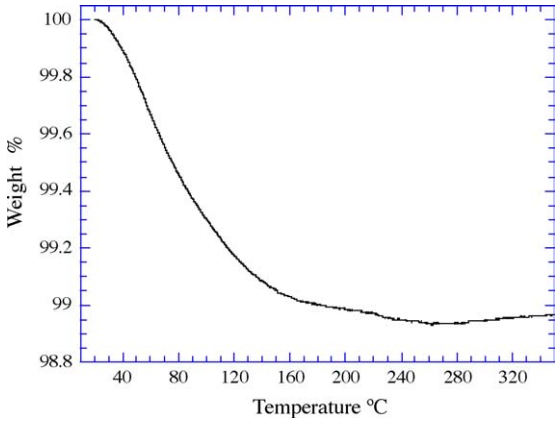

Fig. 6. TGA trace of CdS modified TiO_2 nanotube-array electrode. The sample was prepared at −0.5 V for 30 min, and rinsed under ethanol, acetone and water, dried under N_2 flow. The experiment was performed in N_2, at a heating rate of 1 °C/min to 350 °C and then kept at 350 °C for 60 min.

was heated at a rate of 1 °C/min in an ultra-high purity N_2 atmosphere, from room temperature to 350 °C, dwelling at 350 °C for 1 h. The TGA plot in Fig. 6 showed that total mass loss of ca. 1.04% in the region from room temperature to 250 °C, which is most likely be due to the physical adsorption of water on the sample [33]. From 300 to 350 °C, with a 350 °C dwell time of 60 min, there is no more measurable weight loss. However, two small exothermic peaks are seen in the DSC data at 350 °C (Fig. 7), most likely due to sintering of the CdS nanoparticles [33]. As we will delineate below, the annealing (sintering) of the CdS nanoparticle-layer has a significant influence on the photoelectrochemical response of the samples.

Fig. 8 shows the normalized visible reflectance spectra of a plain TiO_2-nanotube array electrode, as well as CdS modified TiO_2 nanotube-array electrodes. The reflectance onset was determined by linear extrapolation from the inflection point of the curve toward the baseline. From Fig. 8,

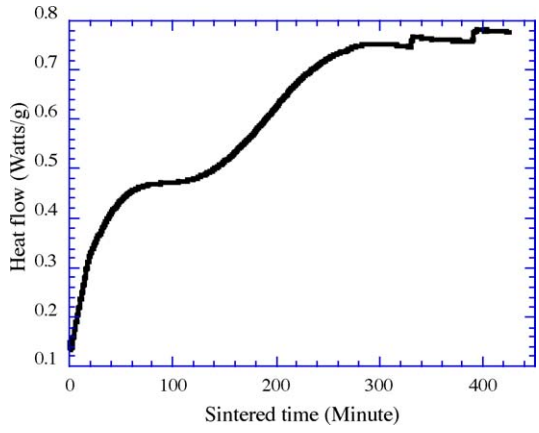

Fig. 7. DTA trace of CdS modified TiO_2 nanotube-array electrode. The sample was prepared at −0.5 V for 30 min, and rinsed under ethanol, acetone and water, dried under N_2 flow.

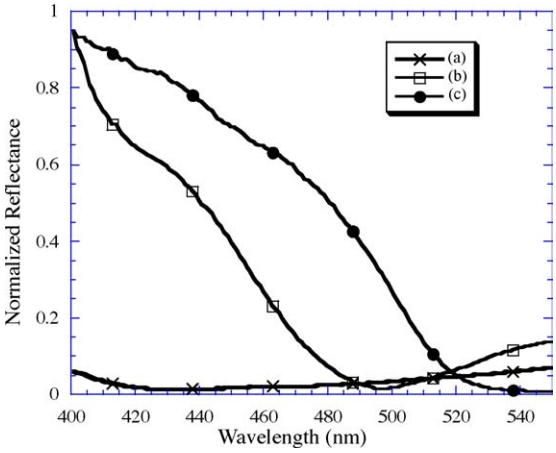

Fig. 8. Normalized visible reflectance spectra of CdS–TiO_2 nanotube-array electrodes. (a): TiO_2 nanotube-array electrode, (b) 20 min −0.5 V electrodeposited CdS modified TiO_2 nanotube-array electrode, as fabricated, (c) electrode of (b) after annealing at 350 °C for 60 min in N_2.

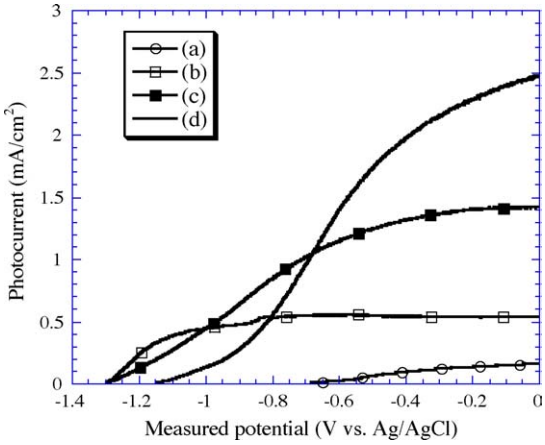

Fig. 9. Photocurrent versus voltage in 1 M Na_2S under AM 1.5 (1 sun), 100 mW/cm^2 illumination: (a) bare TiO_2 nanotube electrode, (b) as-prepared electrodeposited CdS film (−0.5 V, 30 min) upon TiO_2 nanotube-array electrode, (c) CdS (−0.5 V, 30 min.)–TiO_2 electrode after annealing at 350 °C in N_2 for 60 min, (d) CdS (−0.5 V, 30 min)–TiO_2 electrode after annealing at 400 °C in N_2 for 60 min.

one can see that deposition of the CdS film atop the TiO_2 nanotube-array electrode has red-shifted the absorption edge into the visible region, with the absorption tail extending to 500 nm; the bandgap calculated from this reflectance edge is about 2.53 eV. After annealing (N_2, 350 °C, 1 h) its absorption behavior has further red-shifted, with the reflectance tail extending to 515 nm, a calculated edge bandgap of 2.41 eV, a typical bandgap value for bulk CdS. The absorption edge corresponds to a nanoparticle size of approximately 10–20 nm [17,34]. With annealing the CdS particles aggregate, causing the spectrum to red-shift, a behavior previously attributed to the formation of valence-band tail states [35].

3.1. Photoelectrochemical properties

The photoelectrochemical properties of the resulting electrodes were tested as prepared, and after annealing at 350 and 400 °C for 60 min in N_2 atmosphere; for comparison, the properties of CdS electro-deposited onto planar FTO was also measured.

Current–voltage characteristics of the prepared CdS-sensitized TiO_2 nanotube electrodes are presented in Fig. 9 for an illumination intensity of 1 sun (AM 1.5, 100 mW/cm^2). The photoelectrochemical measurements were obtained using a 1 M Na_2S electrolyte solution, an efficient hole scavenger for CdS in which the electrodes are stable. From UV–vis spectra, one knows that a small portion of the CdS–TiO_2 electrode absorption spectrum extends into the visible region. For the as-prepared CdS–TiO_2 electrode (Fig. 9b) photocurrent onset occurs at −1.30 V versus Ag/AgCl, a −0.60 V negative shift compared to the plain TiO_2 nanotube-array electrode. In comparison to the plain TiO_2 nanotube-array electrode addition of the CdS film increased the photocurrent from 0.16 to 0.55 mA/cm^2 and the *I–V* plot of as-prepared sample showed a well-defined photocurrent saturation region (Fig. 9b). Our results show that an electrochemically synthesized CdS thin film comprised of nanoparticles can be used to sensitize the TiO_2 nanotube-array making it more responsive to the visible spectrum, with obvious application to solar cells [15,17,20]. The photocurrent response is sensitive to the annealing temperature, as discernable in Fig. 9c–d. The sample annealed at 350 °C reaches ≈ 1.42 mA/cm^2, and the 400 °C annealed sample reaches ≈ 2.51 mA/cm^2, respectively 9 and 16 times higher than that of bare TiO_2 nanotube array electrode. The *I–V* curves of these samples gradually lose their well-defined photocurrent saturation as the annealing temperature increases. Higher temperature annealing may result in pore blockage due to sintering of the CdS nanoparticles, reducing the area accessible to the hole scavenging electrolyte solution. With respect to the photogenerated holes in the CdS nanoparticles, this will result in a more efficient electron back-reaction in the

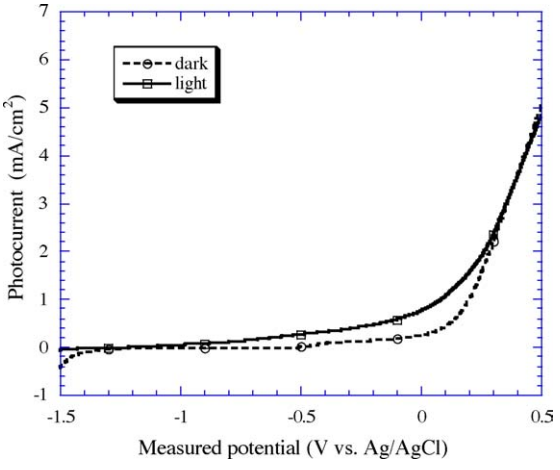

Fig. 10. Photocurrent vs. measured potential for electro-deposited CdS film (−0.5 V, 30 min) a top planar FTO substrate glass after annealing at 400 °C for 60 min.

TiO_2 conduction band leading to non-ideal *I–V* behavior. This premise is confirmed by our *I–V* plot of an electro-deposited CdS-nanoparticle film upon planar FTO, annealed at 400 °C for 60 min, as shown in Fig. 10.

4. Conclusions

A novel electrodeposited CdS nanoparticle modified TiO_2 nanotube-array electrode is presented in this work. The highly-ordered nanotube array is self-assembled by the anodization process [28] without the use of any templates. Investigations via XPS, XRD, TGA-DSC, UV–vis absorption spectra, and FE-SEM showed that sphere-like CdS-nanoparticles, approximately 10–20 nm in diameter, were synthesized by electro-deposition from a non-aqueous solution. Longer electrodeposition times resulted in formation of larger CdS nanoparticle clumps, approximately 40–100 nm in diameter. It was not possible to discern CdS nanoparticles within the nanotubes. The CdS layer significantly extends the response of the TiO_2 nanotube-array electrodes into the visible region. Compared to a plain TiO_2 nanotube array electrode, photoelectrochemical measurements show that the visible light photocurrent increases by a factor of ≈16 with electro-deposition of the CdS layer. The absorption edge corresponds to a nanoparticle size of approximately 10–20 nm [17,34]. With annealing the spectrum red-shifts, a behavior similarly noted in [35] and thought due to the formation of valence-band tail states. High temperature annealing of the CdS layer appears to limit the surface area exposed to the hole-scavenging electrolyte, significantly impacting the *I–V* characteristics of the CdS–TiO_2 photoelectrodes.

References

[1] B. O'Regan, M. Grätzel, A low-cost, high-efficiency solar-cell based on dye-sensitized colloid TiO_2 films, Nature 353 (1991) 737–740.

[2] A. Hagfeldt, M. Grätzel, Light-induced redox reactions in nanocrystalline systems, Chem. Rev. 95 (1995) 49–68.

[3] S.U.M. Khan, M. Al-Shahry, W.B. Ingler Jr., Efficient photochemical water splitting by a chemically modified *n*-TiO_2, Science 297 (2002) 2243–2245.

[4] A.L. Linsebigler, G. Lu, J.Y. Yates, Photocatalysis on TiO_2 surfaces-Principles, mechanisms, and selected results, Chem. Rev. 95 (1995) 735–758.

[5] R.L. Pozzo, M.A. Baltanas, A.E. Cassano, Supported titanium oxide as photocatalyst in water decontamination: State of the Art, Catal. Today 39 (1997) 219–231.

[6] J.-M. Herrmann, Heterogeneous photocatalysis: Fundamentals and applications to the removal of various types of aqueous pollutants, Catal. Today 53 (1999) 115–129.

[7] A. Zaban, S.G. Chen, S. Chappel, B.A. Gregg, Bilayer nanoporous electrodes for dye sensitized solar cells, Chem. Commun. 22 (2000) 2231–2232.

[8] O.K. Varghese, M. Paulose, K.G. Ong, E.C. Dickey, C.A. Grimes, Extreme Changes in the Electrical Resistance of Titania Nanotubes with Hydrogen Exposure, Adv. Mater. 15 (2003) 624–627.

[9] G.K. Mor, K. Shankar, M. Paulose, O.K. Varghese, C.A. Grimes, Enhanced photocleavage of water using titania nanotube-arrays, Nano Lett. 5 (2005) 191–195.

[10] O.K. Varghese, M. Paulose, K. Shankar, G.K. Mor, C.A. Grimes, Water-photolysis properties of highly-ordered titania nanotube-arrays, J. Nanosci. Nanotech. 5 (2005) 1158–1165.

[11] T. Tachikawa, S. Tojo, K. Kawai, M. Endo, M. Fujitsuka, T. Ohno, K. Nishijima, Z. Miyamoto, T. Majima, Photocatalytic oxidation reactivity of holes in the sulfur- and carbon-doped TiO_2 powders studied by time-resolved diffuse reflectance spectroscopy, J. Phys. Chem. B 108 (2004) 19299–19306.

[12] F. Gracia, J.P. Holgado, A. Caballero, A.R. Gonzalez-Elipe, Structural, optical, and photoelectrochemical properties of Mn^+–TiO_2 model thin film photocatalysis, J. Phys. Chem. B 108 (2004) 17466–17476.

[13] H. Gerischer, M. Lubke, A particle size effect in the sensitization of TiO_2 electrodes by a CdS deposit, J. Electroanal. Chem. 204 (1986) 225–227.

[14] R. Vogel, P. Hoyer, H. Weller, Quantum-sized CdS, PbS, CdS, Ag_2S, Sb_2S_3, and Bi_2S_3 particles as sensitizers for various nanoporous wide-bandgap semiconductors, J. Phys. Chem. 98 (1994) 3183–3188.

[15] R. Vogel, K. Pohl, H. Weller, Sensitization of highly porous, polycrystalline TiO_2 electrodes by quantum sized CdS, Chem. Phys. Lett. 174 (1990) 241–246.

[16] S. Kohtani, A. Kudo, T. Sakata, Spectral sensitization of a TiO_2 semiconductor electrode by CdS microcrystals and its photoelectrochemical properties, Chem. Phys. Lett. 206 (1993) 166–170.

[17] P.A. Sant, P.V. Kamat, Interparticles electron transfer between size-quantized CdS and TiO_2 semiconductor nanoclasters, Phys. Chem. Chem. Phys. 4 (2002) 198–203.

[18] R. Flood, B. Enright, M. Allen, S. Barry, A. Dalton, H. Doyle, D. Tynan, D. Fitzmaurice, Determination of band edge energies for transparent nanocrystalline TiO_2–CdS sandwich electrodes prepared by electrodeposition, Sol. Energy Mater. Sol. Cells 39 (1995) 83–98.

[19] Y.G. Guo, J.S. Hu, H.P. Liang, L.J. Wan, C.L. Bai, TiO_2-based composite nanotube arrays prepared via layer-by-layer assembly, Adv. Funct. Mater. 15 (2005) 196–202.

[20] S.G. Hickey, D.J. Riley, E.J. Tuhh, Photoelectrochemical studies of CdS nanoparticles modified electrodes: absorption and photocurrent investigations, J. Phys. Chem. B 104 (2000) 7623–7626.

[21] L.M. Peter, D.J. Riley, E.J. Tull, K.G.U. Wijayantha, Photosensitization of nanocrystalline TiO_2 by self-assembled layers of CdS quantum dots, Chem. Commun. 10 (2002) 1030–1031.

[22] S. Drouard, S.G. Hickey, D.J. Riley, CdS nanoparticles-modified electrodes for photoelectrochemical studies, Chem. Commun. 1 (1999) 67–68.

[23] G.A. Il'chuk, V.O. Ukrainets, Y.V. Rud', O.I. Kuntyi, N.A. Ukrainets, B.A. Lukiyanets, R.Yu. Petrus, Electrochemical synthesis of thin CdS films, Tech. Phys. Lett. 30 (2004) 628–630.

[24] A.V. Feitosa, M.A.R. Miranda, J.M. Sasaki, M.A. Araujo-Silva, A New route for preparing CdS thin films by chemical bath deposition using EDTA as ligand, Braz. J. Phys. 34 (2004) 656–658.

[25] K. Rajeshwar, Electrosynthesized thin-films of group-II–VI compound semiconductors, alloys and superstructures, Adv. Mater. 4 (1992) 23–29.

[26] G. Hodes, Physical Electrochemistry, Marcel Dekker, New York, 1995.

[27] R.K. Pandey, S.N. Sahu, S. Chandra, Handbook of Semiconductor Electrodeposition, Marcel Dekker, New York, 1996.

[28] D.W. Gong, C.A. Grimes, O.K. Varghese, W. Hu, R.S. Singh, Z. Chen, E.C. Dickey, Titanium oxide nanotube arrays prepared by anodic oxidation, J. Mater. Res. 16 (2001) 3331–3334.

[29] M. Kundu, A.A. Khosravi, S.K. Kulkarni, Synthesis and study of organically capped ultra small clusters of cadmium sulphite, J. Mater. Sci. 32 (1997) 245–258.

[30] K. Bandyopadhyay, K.S. Mayya, K. Vijayamohanan, M. Sastry, Spontaneously organized molecular assembly of an aromatic organic disulfide on silver/platinum alloy surfaces: an angle dependent X-ray photoemission investigation, J. Electr. Spectrosc. 87 (1997) 101–107.
[31] M. Savelli, J. Bougnot, in: B.O. Seraphim (Ed.), Topics in Applied Physics, 31, Solar Energy Conversion, Springer Verlag, Berlin, 1979.
[32] O.K. Varghese, D.W. Gong, M. Paulose, C.A. Grimes, E.C. Dickey, Crystallization and high-temperature structural stability of titanium oxide nanotube arrays, J. Mater. Res. 18 (2003) 156–165.
[33] A. Kumar, A.B. Mandale, M. Sastry, Phase transfer of aqueous CdS nanoparticles by coordination with octadecanetthiol molecules present in non-polar organic solvents, Langmuir 16 (2000) 9299–9302.
[34] A. Henglein, Small-particle research: Physical chemical properties of extremely small colloidal metal and semiconductor particles, Chem. Rev. 98 (1989) 1861–1873.
[35] J. Kokai, A.E. Rakhshani, Photocurrent spectroscopy of solution-grown CdS films annealed in $CdCl_2$ vapour, J. Phys. D Appl. Phys. 37 (2004) 1970–1975.